Heat Generation Effect on Three-Dimensional Couple Stress Casson Liquid Motion via Stretching Sheet

C. Srinivasulu[1], D. Yasoda[2], Ashfar Ahmed[3], B. Madhusudhana Rao[4]

[1]Department of Mathematics, Humanities and Basic Sciences, Annamacharya Institute of Technology and Sciences, Karkambadi Road, Tirupati-517520, A.P, India

[2] Department of Mathematics, Humanities and Basic Sciences, Annamacharya Institute of Technology and Sciences, Karkambadi Road, Tirupati-517520, A.P, India

[3]Assistant Professor, Department of Mathematics, Malla Reddy Engineering College (Autonomous), Medchal, Secunderabad-500100, Telangana, India

Department of Information technology, Faculty of mathematics, University of technology and Applied Sciences, Muscat, Oman

Abstract:

The numerical analysis of Heat generation Effect on 3D CSC (Couple Stress Casson) liquid motion via stretching sheet. The set of PDE are translated into ODE's form by help of similarity variables. The numerical methodology by help of shooting technique is explore into numerical solutions based on MATLAB programming. The solutions of various physical parameters are explained through graphically in the form of velocity, temperature and concentration profiles. Moreover, the skin friction coefficient along x^*, y^* directions, heat and mass transfer rates. It is observed that the couple stress non-Newtonian liquid motion over stretching surface has produce more HMTR (Heat and Mass Transfer Rate) when presence of β^*, K_1 (Casson parameter, Couple stress parameter respectively).

Key words: Heat Source; Casson Fluid; Chemical Reaction; MHD; Couple Stress.

Introduction:

The investigation of heat transfer and mass effects on MHD motion has attracted considerable attention in research due to its relevance in various industrial and engineering applications. These applications span a wide range, including geothermal energy extraction, nuclear reactors, plasma studies, and MHD generators. Researchers focus on studying the behavior of electrically conducting, viscous, and incompressible fluids to better understand and optimize these processes. Both the polymer and biomechanics industries depend significantly on Casson fluids. Rekha Deva and Sood et al. [1] develop the analysis of heat transfer properties of a Casson liquid with magnetic field via exponentially stretched surface. Khadija et al. [2] analysed Casson liquid containing carbon nanotubes of various lengths and radii on moving porous plate. The MHD free convection flow of Casson liquid with thermal radiation via vertical porous channel was investigation by Ojemeri et al. [3]. The non-Newtonian Casson fluid squeezed between two parallel plates is performed under the influence of MHD and Darcian effects was investigated Mubashir et al. [4]. The unsteady MHD Casson fluid flow via an oscillating inclined plate is investigated by Parismita et al. [5]. Mohamad et al. [6] examined numerical investigations of the influence of Peclet number on Casson liquid convective motion via horizontal porous layer.

The importance of heat and mass transfer in non-Newtonian fluids is significant due to their widespread applications in various industries such as plastics, pharmaceuticals, thermal technology, lubricants, and bitumen products. These fluids exhibit complex flow behavior that requires a deep understanding of their rheological properties for efficient design and process optimization. Among the various theories describing the behavior of non-Newtonian fluids, Stokes [8] introduced a nonlinear rheological model. This model establishes a relationship between stress and strain, which is crucial for predicting and managing the behavior of non-Newtonian fluids under different processing conditions. Salahuddin and Awais [9] investigated the heat and mass transfer rate with Cattaneo-Cristov model for the 2D MHD couple stress liquid motion in a sensory surface. Saqib et al. [10] studied fractal fractional order derivative operators are highly sophisticated mathematical tools that can be applied in a variety of physics and engineering situations.

Mathematical Formulation:

The effect of heat generation on 3D Casson couple stress fluid motion via stretching surface was consider at $z=0$. In the direction of z, we applied magnetic field M_0 and perpendicular to the surface (i.e. $x^* y^*$-plane) with electrically conducting. The liquid motion occupies the region $z>0$ as it displayed in **Fig. 1**. The stretching velocities

$u = U_w(\mathrm{x}) = ax,\ v_1 = V_w(\mathrm{y}) = by$. The established rheological equation of isotropic and steady Casson liquid motion as:

$$\tau_{ij}^* = \begin{cases} \left(2\mu_0^* + \dfrac{2p_y^*}{\sqrt{2\pi^*}}\right)e_{ij}, & \pi^* \geq \pi_1^* \\ \left(2\mu_0^* + \dfrac{2p_y^*}{\sqrt{2\pi_1^*}}\right)e_{ij}, & \pi^* < \pi_1^* \end{cases} \tag{1}$$

Where, $\pi^* = e_{ij}e_{ij}$ and $p_y^* = \mu_0^*\sqrt{2\pi^*} / \beta^*$ with the consideration. The established governing equations continuity, heat and concentration equations for the boundary layer motion as taken following forms:

$$\frac{\partial u}{\partial x} + \frac{\partial v}{\partial y} + \frac{\partial w}{\partial z} = 0 \tag{2}$$

$$u\frac{\partial u}{\partial x} + v\frac{\partial u}{\partial y} + w\frac{\partial u}{\partial z} = \upsilon\left(1 + \frac{1}{\beta}\right)\frac{\partial^2 u}{\partial(z)^2} - (\upsilon)'\frac{\partial^4 u}{\partial(z)^4} - \frac{\sigma M_0^2}{\rho}u \tag{3}$$

$$u\frac{\partial v}{\partial x} + v\frac{\partial v}{\partial y} + w\frac{\partial v}{\partial z} = \upsilon\left(1 + \frac{1}{\beta}\right)\frac{\partial^2 v}{\partial(z)^2} - (\upsilon)'\frac{\partial^4 v}{\partial(z)^4} - \frac{\sigma M_0^2}{\rho}v \tag{4}$$

$$u\frac{\partial T}{\partial x} + v\frac{\partial T}{\partial y} + w\frac{\partial T}{\partial z} = \alpha_m\frac{\partial^2 T}{\partial(z)^2} - \frac{Q_0}{(\rho \mathrm{C})_f}(\mathrm{T} - \mathrm{T}_\infty) \tag{5}$$

$$u\frac{\partial C}{\partial x} + v\frac{\partial C}{\partial y} + w\frac{\partial C}{\partial z} = D\frac{\partial^2 C}{\partial(z)^2} \tag{6}$$

The relevant boundary conditions of the present model as

$$\begin{aligned} &u = ax,\ \ \mathrm{v} = by,\ \ \mathrm{w} = 0,\ \ -k\frac{\partial T}{\partial z} = h_1(\mathrm{T}_f - \mathrm{T}),\ \ -D\left(\frac{\partial C}{\partial z}\right) = h_2\left(C_f - C\right),\ \text{at}\ \ \mathrm{z} = 0 \\ &u \to 0,\ \ v \to 0,\ \ u' \to 0,\ \ v' \to 0,\ T \to T_\infty,\ \ C \to C_\infty,\ \ as\ \ \ z \to \infty \end{aligned} \tag{7}$$

The similarity transformations as below

$$\left.\begin{aligned} &\eta_1 = \sqrt{\frac{a}{\upsilon_f}}z,\quad u_1 = axf'(\eta),\quad v = ayg'(\eta),\quad \mathrm{w} = -\sqrt{a\upsilon}(f(\eta) + g(\eta)) \\ &\qquad \theta(\eta) = \frac{T - T_\infty}{T_w - T_\infty},\quad \phi(\eta) = \frac{C - C_\infty}{C_w - C_\infty} \end{aligned}\right\} \tag{8}$$

Using above **Eq. (8)**, we are converting **Eq. (3)-(6)** into below format

$$K_1 f^{v} + M_1 f' - f'''(1+\frac{1}{\beta^*}) - f''(f+g) + (f')^2 = 0 \tag{9}$$

$$K_1 g^{v} + M_1 g' - g'''(1+\frac{1}{\beta^*}) - g''(f+g) + (g')^2 = 0 \tag{10}$$

$$\theta'' + \Pr(f+g)\theta' - H_1 \Pr\theta = 0 \tag{11}$$

$$\phi'' - \Pr Le\left((f+g)\phi' + \gamma^*\phi\right) = 0 \tag{12}$$

Corresponding B.Cs as below

$$\left.\begin{array}{l} \eta_1 = 0 \ \ as \ \ f=0, \quad g=0, \quad f'=1, \quad g'=\lambda^*, \quad \theta' = -\gamma_1(1-\theta), \ \ \phi' = -\gamma_2(1-\phi) \\ \eta_1 \to \infty \ \ at \ \ f' \to 0, \ \ g' \to 0, \ \ f'' \to 0, \ \ g'' \to 0, \ \ \theta \to 0, \ \ \phi \to 0, \end{array}\right\} \tag{13}$$

Moreover the skin-friction coefficient and Nusselt number are below

$$\left.\begin{array}{l} \mathrm{Re}_x^{1/2} C_{fx} = (1+\beta^*/\beta^*) f''(0) - K_1 f^{v}(0), \ \ \mathrm{Re}_x^{1/2} C_{fy} = (1+\beta^*/\beta^*) g''(0) - K_1 g^{v}(0) \\ \mathrm{Re}_x^{-1/2} Nu_x = -\theta'(0), \ \ \mathrm{Sh}\mathrm{Re}_x^{-1/2} = -\phi'(0) \end{array}\right\} \tag{14}$$

Results and Discussion:

The couple stress Casson fluid characteristics of λ^* on velocity motion along x^*, y^*-axis $\left(f'(\eta_1), g'(\eta_1)\right)$ as illustrated respectively in **Figure 2**. It is perceived that, the $f'(\eta_1), g'(\eta_1)$ convergence (point at surface area is $\lambda^* = 0.8$ (not exact value)) monotonically increases along with x^*, y^* axis and associated boundary layer thickness of couple stress non-Newtonian fluid motion is thinner with ascending numerical values of λ^*. **Figure 3** predicts the effect of K_1 on $\theta(\eta_1)$. It is analysed that, the speed of non-Newtonian liquid is decreases $\theta(\eta_1)$ for distinct enlarge values of K_1.

The most significant characteristic M_1 (Magnetic field parameter) on $f'(\eta_1), g'(\eta_1)$ respectively presented in **Figs. 4-5**. It is dictated that, the velocity in y^*- axis $g'(\eta_1)$ is high convergence deference than the x^*-axis velocity $f'(\eta_1)$ and also $\mathrm{Re}_x^{1/2} C_{fx}$ rises in fluid motion along in x^*, y^*-axis with growth numerical values of M_1.

The variation of H_1 (heat absorption parameter) on $\mathrm{Re}_x^{-1/2} Nu_x$ for Casson couple stress fluid and pure fluid as expressed in **Fig. 6**. The heat transfer $\left(\mathrm{Re}_x^{-1/2} Nu_x\right)$ is high with enlarge values of H_1. It is clear view of $\mathrm{Re}_x^{-1/2} Nu_x$ is more effected in Pure fluid while comparison of Casson couple stress fluid (non-Newtonian couple stress fluid). Characterise of Le (Lewis number) with absence and presence of Casson fluid and absence of Casson fluid on $\mathrm{Sh}\,\mathrm{Re}_x^{-1/2}$ displays in **Fig. 7**. In view of this the $\mathrm{Sh}\,\mathrm{Re}_x^{-1/2}$ profile enlarges with distinct ascending values of Le. It is finally Conclude that, the couple stress fluid is Produce high mass transfer rate while comparing Casson couple stress fluid.

Conclusion

This work we have deals with the heat source effect on 3D convective flow of non-Newtonian couple stress fluid over bidirectional stretching surface with chemical reaction. The significant results noticed as follows:

- The velocity of Casson fluid and heat transfer rate is very high for hydromagnetic $M_1 > 0$ case.
- The heat transfer rate $Nu_x \mathrm{Re}_x^{-1/2}$ generate more in pure fluid $(\beta = K \to \infty)$ with enlarge values of H_1.

References

1. Devi R, Sood S, Numerical Analysis of the Influence of an Inclined Magnetic Field on the Flow of Casson Nanofluid Across an Exponentially Stretching Surface, using the Darcy-Forchheimer model. Indian Journal of Science and Technology 16(44) (2023) 4081-4089. https://doi.org/10.17485/IJST/v16i44.2481.
2. R. Khadija, M. Zafar, Adnan, K. Umar, A. Bilal, F.A. Awwad and E.A. A. Ismail, Numerical analysis of non-linear radiative Casson fluids containing CNTs having length and radius over permeable moving plate, open Physics, (2024). https://doi.org/10.1515/phys-2024-0013.
3. G. Ojemeri, E. Omokhuale, M.M. Hamza, I.O. Onwubuya, A. Shuaibu, A Computational Analysis on Steady MHD Casson Fluid Flow Across A Vertical Porous Channel Affected By Thermal Radiation Effect, International Journal of Science for Global Sustainability, 9(1) (2023). DOI: https://doi.org/10.57233/ijsgs.v9i1.393.
4. Q. Mubashir, A. Sidra and A. Efaza, Fractional Modeling of Non-Newtonian Casson Fluid between Two Parallel Plates, Journal of Mathematics, e12727 (2023) 1-12. https://doi.org/10.1155/2023/5517617.

5. P. Parismita, D. Hiren and H. Puja, Numerical Analysis of Entropy Generation of MHD Casson Fluid Flow Through an Inclined Plate with Soret Effect, East European Journal of Physics, 2 (2024). DOI: https://doi.org/10.26565/2312-4334-2024-2-18.
6. A.M. Mohamad, Y. Dhananjay, N. Sanjith Bharatharajan, A. Mukesh Kumar, R. Ravi and K. Bhattacharyya, The effect of Péclet number on the onset of Casson fluid convective motion in a porous layer: Analytical and numerical investigations, Numerical Heat Transfer, Part B: Fundamentals, (2024). https://doi.org/10.1080/10407790.2024.2320720.
7. M. T. Rehman Siddiqi, M. Safdar, H.M. Dutt, S. Taj, M. Ijaz Khan, B.S. Abdullaeva, R. Altuijri, A.M. Hassan, Comparative analysis of analytical and numerical approximations for the flow and heat transfer in mixed convection stagnation point flow of Casson fluid, Results in Physics, 52 (2023) 106819. https://doi.org/10.1016/j.rinp.2023.106819.
8. V.K. Stokes, Couple Stresses in Fluids. In: Theories of Fluids with Microstructure. Springer, Berlin, Heidelberg, (1984) 34-80. https://doi.org/10.1007/978-3-642-82351-0_4.
9. T. Salahuddin, M and Awais, Cattaneo-Christov flow analysis of unsteady couple stress fluid with variable fluid properties: By using Adam's method, Alexandria Engineering Journal, 81 (2023) 64-86. https://doi.org/10.1016/j.aej.2023.09.021.
10. M. Saqib Murtaza, A. Zubair, E.A. Ibn, Z. Akhtar, T. Fairouz, A. Hijaz, W. Y. Shao, Analysis and numerical simulation of fractal-fractional order non-linear couple stress nanofluid with cadmium telluride nanoparticles, Journal of King Saud University - Science, 35(4) (202) 102618.

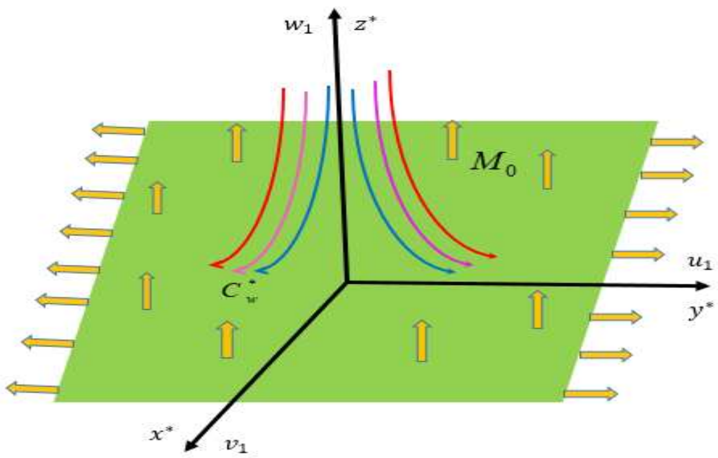

Fig. 1 Physical modeling of the problem

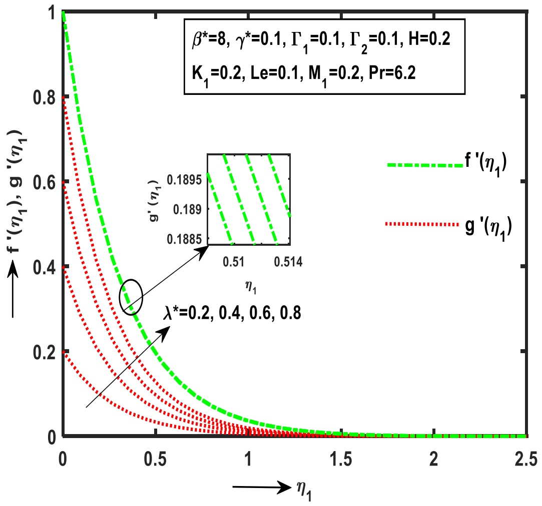

Fig. 2 Effect of λ^* on $f'(\eta_1)$, $g'(\eta_1)$

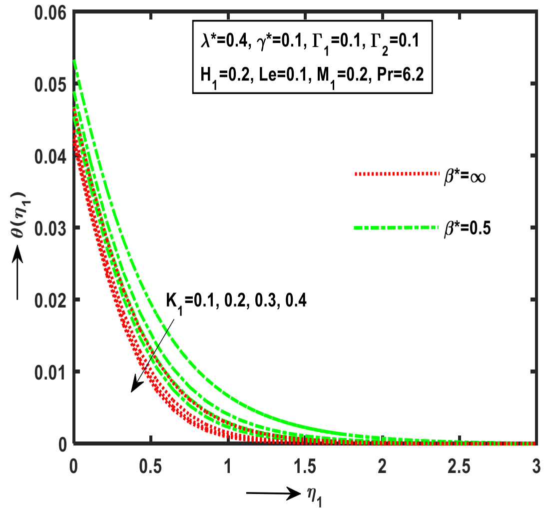

Fig. 3 Effect of K_1 on $\theta(\eta_1)$

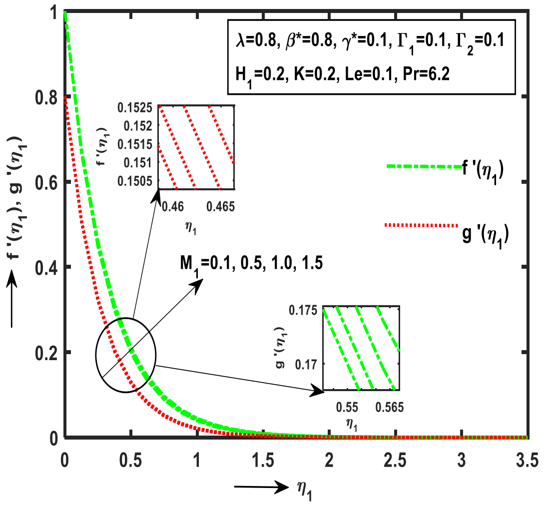

Fig. 4 Effect of M_1 on $f'(\eta_1)$, $g'(\eta_1)$

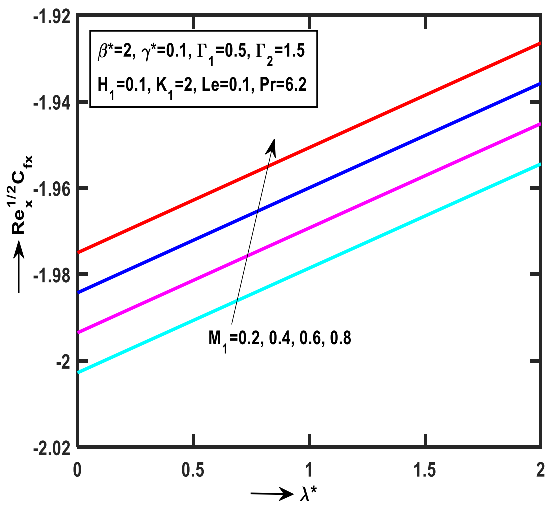

Fig. 5 Effect of M_1 on $\mathrm{Re}_x^{1/2} C_{fx}$

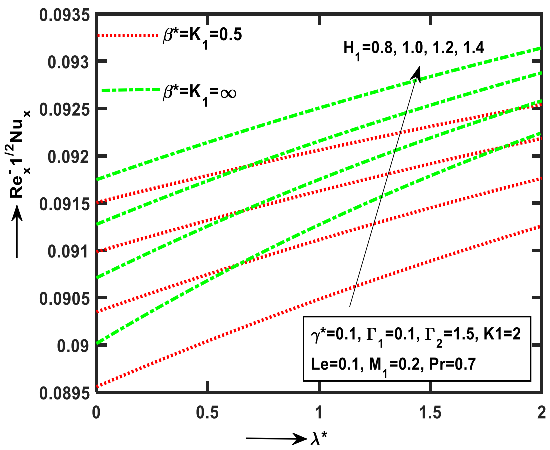

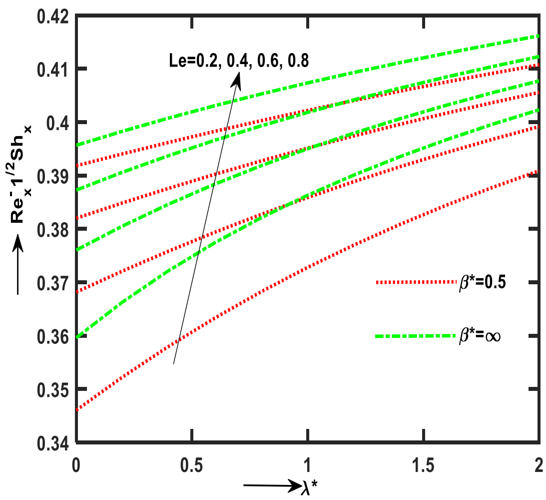

Fig. 6 Effect of H_1 on $Nu_x \mathrm{Re}_x^{-1/2}$ **Fig. 7** Effect of Le on $\mathrm{Sh}\,\mathrm{Re}_x^{-1/2}$

Nomenclature	
a_1 Channel length	τ_w wall shear stress
b_1 Thermal slip parameter	(u_1, v_1) Velocity components along x^*, y^* axis
u_1, v_1, w_1 velocity components along x^*, y^*, z^*	(x^*, y^*) Cartesian coordinate's
C^* Nanoparticle volume fraction	U_w^* Stretching velocity
C_∞^* Uniform ambient concentration	U_∞^* Free stream velocity
C_f^* Skin friction coefficient	***Greek symbols***
C_w^* Variable concentration	ϕ Dimensionless concentration
D_T Thermophoresis diffusion	λ^* Ratio parameter $= b_1/a_1$
D_B Brownian diffusion	υ^* Kinematic viscosity $= \mu/\rho_f$
f Dimensionless stream function	σ^* Boltzmann constant
f' Dimensionless velocity	θ Dimensionless temperature
K_1 Couple Stress Parameter $= \dfrac{a_1(\upsilon^*)'}{(\upsilon^*)^2}$	Γ_1, Γ_2 Temperature and concentration Biot Numbers respectively
Le Lewis number $= \dfrac{\alpha_m^*}{D_B}$	$(\upsilon^*)'$ Couple stress viscosity $= n/\rho_f$
M_1 Magnetic field parameter $= \dfrac{\sigma^* M_0^2}{a_1 \rho_f}$	ρ Fluid density
Pr Prandtl number $= \left(\dfrac{\upsilon^*}{\alpha_m^*}\right)$	ρ_f Fluid density
Re_x Reynolds number	α_m^* thermal diffusivity $= k/(\rho C)_f$
$\mathrm{Re}_x^{-1/2} Nu_x$ Heat Transfer Rate	$\mathrm{Sh}\,\mathrm{Re}_x^{-1/2}$ Mass Transfer Rate
T^* Fluid temperature	η_1 Similarity variable
T_1^* Temperature on lower wall	μ Dynamic viscosity
T_2^* Temperature on upper wall	***Subscripts***
T_∞^* fluid temperature far away from the surface	∞ condition at free stream
T_w^* Constant fluid Temperature of the wall	w wall mass transfer velocity